Petroleum & Coal
ISSN 1337-7027

Available online at www.vurup.sk/pc
Petroleum & Coal 51 (4) 260-269, 2009

STATISTICAL ANALYSIS OF GEOCHEMICAL DISTRIBUTION OF MAJOR AND TRACE ELEMENTS OF THE MAASTRICHTIAN COAL MEASURES IN THE ANAMBRA BASIN, NIGERIA

Jude E. Ogala[*1], Mike I. Akaegbobi[2], Omolemo O. Omo-Irabor[1], and Robert B. Finkelman[3]

[1]*Department of Geology, Delta State University, Abraka, Nigeria.,*
[2]*Department of Geology, University of Ibadan, Ibadan, Nigeria.,*
[3]*Department of Geosciences, The University of Texas at Dallas, Richardson, TX 75080, USA,* *Correspondence author email: etunimogala@yahoo.com

Received August 8, 2009, December 1, 2009

Abstract

This work establishes through statistical analyses the relationship that exists among the major and trace elements in the Maastrichian Coal Measures of Southeastern Nigeria. Laboratory analyses were performed using the inductively coupled plasma-optical emission spectrometry (ICP-OES). Two distinct populations were deduced; the first population represents rocks from a detrital suite dominated by quartz and clay minerals. The second suite comprises the coal samples deposited in the peat swamp. These suites are unrelated because there is no transition from one to the other. The geological interpretation of factors/components yields insight into the association of major and trace elements in the rocks of the Maastrichtian coal measures and main phases that govern the distribution of geochemical variables.

Keywords: Coal Measures, Geochemistry, Factor analysis, Principal component analysis, Anambra Basin, Nigeria

1. Introduction

The Anambra Basin comprises mainly of sedimentary rocks (sandstones, siltstones, mudstones and shales) and occupies the lower section of the Benue Trough. The basin is richly endowed with sub-bituminous coal seams which are found within the Mamu and Nsukka Formations of Campanian-Maastrichtian age. A number of studies have concentrated on the stratigraphic sequence of the Anambra Basin [1-3]. There has been limited number of research work in terms of utilizing the major and trace elements present in the sediments of the Coal Measures, to determine the processes responsible for their geochemical distribution.

A number of authors have concentrated mainly on the abundance and distribution of elements in the Nigerian coal. For instance, [4] determined major, minor, and trace elements in three Nigerian coals (Okpara, Onyema and Ekulu mines) [5], analysed 24 samples from the Enugu coal deposit for eleven elements using the Particle Induced X-ray Emission (PIXE) and Rutherford Backscattering (RBS) techniques [6], compared the quality of coal (raw and washed), coke char, coke, and briquettes from eight Nigerian mines (Onyeama, Ogbete, Enugu, Gombe, Asaba-Ogwashi, Okaba, Afikpo and Lafia) using cluster analysis [7], analyzed the metal contents and concentrations of an unspecified number of Nigerian coal samples using atomic absorption spectrophotometer (AAS). By employing (lithium metaborate/tetraborate fusion), inductively coupled plasma optical emission mass spectrometry (ICP-OES), combustion infra-red (LECO) and modified acid-base accounting, [8] investigated the potential of the coal and coal-bearing units of the Lower, Middle and Upper Benue Trough to produce acid mine drainage conditions [9], applied epithermal neutron activation (ENAA) in combination with principal component analysis

(PCA) to determine the distribution of major and trace elements in igneous and metamorphic rocks.

This study utilizes fusion-inductively coupled plasma (FUS-ICP) and total digestion - inductively coupled plasma (TD-ICP) for the analysis of 38 elements. The aim of this study is to determine the relationships that exist among the major and trace elements of the Nigerian Coal Measures through statistical analysis.

2. Stratigraphy

The Anambra Basin was formed during the Santonian folding and uplift, that left a prominent synclinal structure in the Lower Benue Trough. The stratigraphic succession ranges from Late Santonian to Eocene (Figure 1), with sediments of fluvial, deltaic, pro-delta and shelf facies origin. The oldest sediments of the basin belong to Nkporo Shales of shallow water origin. The Coal Measures are Maastrichtian and represent a period of non-marine sedimentation at the end of the Cretaceous [3]. The lithology of the Coal Measures consists of alterations of sandstones, siltstones, mudstones and shales with concretionary siderite and marcasite [3]. In the early Paleocene, the Nsukka Formation was deposited. According to [2], the Nsukka Formation, which overlies the Ajali Sandstone, begins with coarse- to medium-grained sandstones and passes upward into well-bedded blue clays, fine-grained sandstones, and carbonaceous shales with thin bands of limestone. The Imo Formation consists of blue-grey clays and shales and black shales with bands of calcareous sandstone, marl, and limestone [2].

PERIOD/AGE		FORMATION
Tertiary	Eocene	Bende/Ameki Formation
	Palaeocene	Imo Shale Group
Cretaceous	Maastrichian - Palaeocene	Nsukka Formation
	Maastrichian	Ajali Formation Mamu Formation
	Campanian - Maastrichian	Enugu/Nkporo /Owelli Formation
	Santonian	

Major Unconformity

Figure 1: Stratigraphic sequence of the Anambra Basin

3. Methods of analysis

3.1 Sampling and laboratory analytical procedures

70 core samples were collected from 11 boreholes in the Anambra Basin from the Nigerian Geological Survey Agency (NGSA), Kaduna, Nigeria (Figure 2). The samples collected from the Upper Cretaceous units in the Anambra Basin include sandstones, siltstones, shales, silty shales with interbedded coal seams (Figure 3). They are generally fine to very fine grained, grey to dark grey with a few whitish calcareous and silty samples. On the whole, 38 parameters were analysed consisting of 10 major elements, loss on ignition (LOI) and 27 trace elements. Laboratory analyses were performed at the Activation Laboratories, Ontario, Canada, using the inductively coupled plasma-optical emission spectrometry (ICP-OES). LOI was determined by weighing before and after ignition at 1050°C.

The fusion technique was used for analysis of major elements and selected trace elements (Table 1). The samples were mixed with a flux of lithium metaborate and lithium tetraborate and fused in an induction furnace. The molten melt is immediately poured into a solution of 5% nitric acid containing an internal standard and mixed continuously until completely dissolved (approximately 30 minutes). The samples were assayed for major oxides and selected trace

elements on a combination fusion technique followed by ICP-OES analysis using a Thermo Jarrel Ash Enviro II simultaneous/sequential ICP.

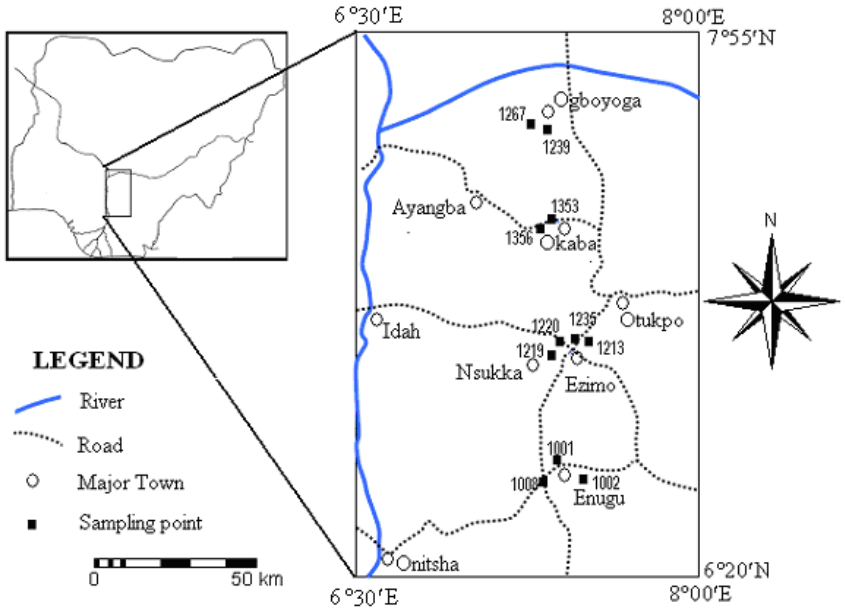

Figure 2: Location of study area with sampling sites

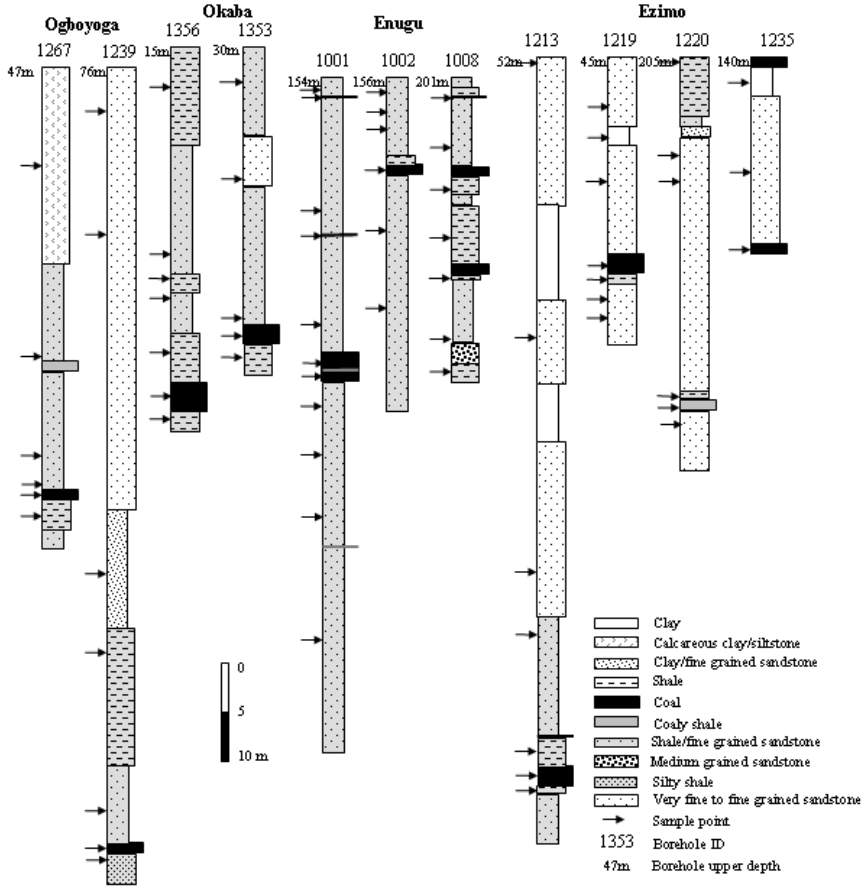

Figure 3: Lithologic sections of sampled boreholes

Table 1 Analytical methods used for major and trace elements analysed and detection limits

Element N=70	Unit Symbol	Detection Limit	Analysis method	Element N=70	Unit Symbol	Detection Limit	Analysis method
SiO_2	%	0.01	FUS-ICP	Ag	ppm	0.3	TD-ICP
Al_2O_3	%	0.01	FUS-ICP	As	ppm	3	TD-ICP
Fe_2O_3T	%	0.01	FUS-ICP	B	ppm	1	TD-ICP
MnO	%	0.001	FUS-ICP	Bi	ppm	2	TD-ICP
MgO	%	0.01	FUS-ICP	Cd	ppm	0.3	TD-ICP
CaO	%	0.01	FUS-ICP	Co	ppm	1	TD-ICP
Na_2O	%	0.01	FUS-ICP	Cr	ppm	1	TD-ICP
K_2O	%	0.01	FUS-ICP	Cu	ppm	1	TD-ICP
TiO_2	%	0.001	FUS-ICP	Ga	ppm	1	TD-ICP
P_2O_5	%	0.01	FUS-ICP	Hg	ppm	1	TD-ICP
LOI	%	0.01	FUS-ICP	Mo	ppm	1	TD-ICP
Total	%	0.01	FUS-ICP	Ni	ppm	1	TD-ICP
Ba	ppm	2	FUS-ICP	Pb	ppm	3	TD-ICP
Sr	ppm	2	FUS-ICP	Sb	ppm	5	TD-ICP
Y	ppm	1	FUS-ICP	S	%	0.01	TD-ICP
Sc	ppm	1	FUS-ICP	Te	ppm	2	TD-ICP
Zr	ppm	2	FUS-ICP	Tl	ppm	5	TD-ICP
Be	ppm	1	FUS-ICP	U	ppm	10	TD-ICP
V	ppm	5	FUS-ICP	W	ppm	5	TD-ICP
				Zn	ppm	1	TD-ICP

For trace element analysis, 0.25 g of the sample was digested with four acids beginning with hydrofluoric, followed by a mixture of nitric and perchloric acids, heated using precise programmer controlled heating in several ramping and heating cycles which takes the samples to dryness. After dryness is attained, samples are brought back into solution using hydrochloric acid. The sample solution was then analysed for elemental concentration using a Varian Vista Pro inductively coupled plasma-optical emission spectrometry (ICP-OES). Calibration was performed using USGS and CANMET certified reference materials.

3.2 Statistical Analysis

The elements were subjected to univariate (minimum, maximum, mean and standard deviation, correlation coefficient) and multivariate (factor and principal component analyses) statistical analysis with the aid of the SPSS 16.0 for Windows (SPSS Inc., Chicago, IL, USA, 2007). Since most of the measured parameters were not normally distributed, the Spearman's rank correlation was used to examine the correlation between elements. The correlation coefficient matrix measures how well the variance of each constituent can be explained by relationship with each other. Factor analysis (FA)/Principal Component Analysis (PCA) were applied on experimental data standardized through z-scale transformation in order to avoid misclassification due to differences in the units of measurement. Standardization tends to increase the influence of variables whose variance is small and reduce the influence of variables whose variance is large [10].

4. Results and Discussion

4.1 Major elements

Table 2 summarises univariate statistics, performed on the measured parameters in terms of their minimum, maximum, mean and standard deviations (S.D.). Samples with minimum values below the detection limit (D.L.) were replaced with half the value of the detection limit and applied for further data processing. Results obtained for samples of 10 major elements shows that SiO_2, Al_2O_3 and Fe_2O_3T account over 75% composition (Table 2). This is in general agreement with

the results from previous work in the Benue Trough [8]. The high concentration of SiO_2 and Al_2O_3 indicate high detrital quartz and clay mineral content in the rocks of the Coal Measures.

The data set was screened to identify outliers. This was achieved by the evaluation of the elements displayed in boxplots (Figures 4 and 5). With the exception of SiO_2, Al_2O_3, Na_2O and K_2O the other measured elements were not normally distributed, therefore the non-parametric Spearman's which applies the ranking order of variables was utilized in the determination of the correlation coefficient.

Table 2 Descriptive Statistics of major elements

Variable N=70	Min	Max	Mean	S.D.
		%		
SiO_2	1.02	96.41	62.18	27.11
Al_2O_3	0.66	30.90	11.24	7.86
Fe_2O_3T	0.04	20.54	1.91	2.81
MnO*(3)	0.0005	0.54	0.03	0.07
MgO*(4)	0.005	0.64	0.14	0.12
CaO* (3)	0.005	0.23	0.05	0.05
Na_2O	0.03	0.16	0.09	0.03
K_2O*(7)	0.005	2.50	0.71	0.69
TiO_2	0.093	3.96	1.26	0.80
P_2O_5*(7)	0.005	0.24	0.06	0.04
LOI	0.69	97.30	21.94	28.06

** Variables with samples below D.L., Min value is half the D.L value*
( ) Number of samples below D.L.

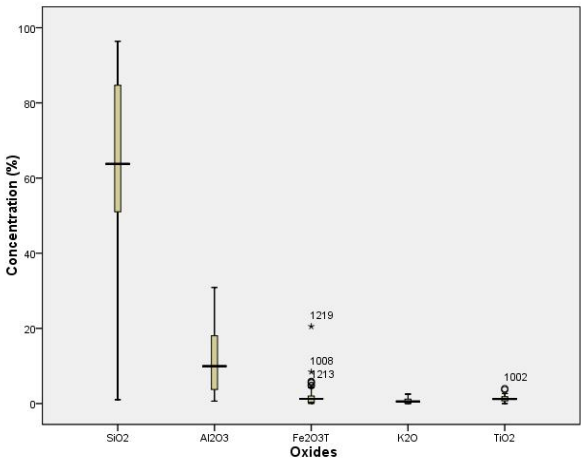

Figure 4 Boxplot of oxides with concentration range of > 1%

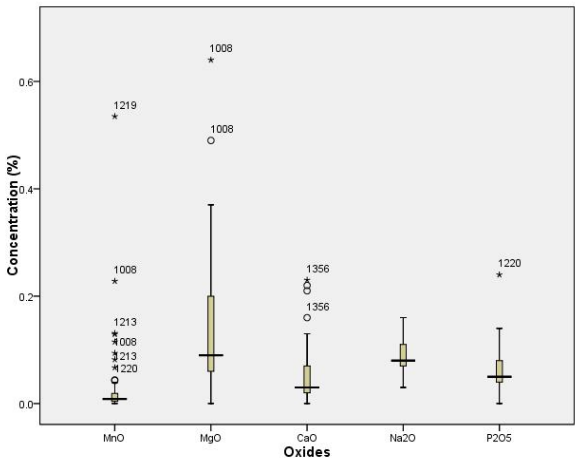

Figure 5 Boxplot of oxides with concentration range of < 1%

Correlation matrix aids in identifying association between variables on a general basis (Table 3). A probability value of $p = 0.05$ was considered as statistically significant in this study. One interesting feature of the correlation matrix is the lack of correlation between SiO_2 and Al_2O_3 indicating that much of the SiO2 is not associated with the Al_2O_3. This is probably due to the fact that much of the SiO_2 is present as quartz. This interpretation is supported by the exceptionally high SiO_2 values and also by a strong correlation between SiO_2 and ash yield. The low and negative correlation of SiO_2 with Al_2O_3 (r=-0.330) and Fe_2O_3T (r=-0.260) imply the occurrence of these oxides in different rock types. The correlation matrix was further subjected to multivariate statistical analysis to provide a better understanding with respect to the relationship existing among elements and the probable processes responsible for their formation.

Factor analysis was performed on the correlation matrix for the major elements of the different sites. This was to identify the relationship among the measured elements. The variance/covariance

and factor loadings of the variables with eigenvalues were therefore computed (Table 4). There appeared to be overlaps among the factors thereby necessitating further analysis. This was achieved by rotation of the axis producing a new set of factors. This was attained after 5 iterations. Each factor involved a sub set of the original variables with as much as possible minimal overlap (Table 5). Since the differences between the unrotated and rotated components were significantly different, the rotated option was used for further analysis. The components were further sorted with the exclusion of values less than 0.500.

Table 3 Correlation matrix of major elements

	SiO_2	Al_2O_3	Fe_2O_3T	MnO	MgO	CaO	Na_2O	K_2O	TiO_2	P_2O_5
SiO_2	1.000									
$Al2O_3$	-0.330	1.000								
Fe_2O_3T	-0.260	0.592	1.000							
MnO	0.163	0.396	0.818	1.000						
MgO	-0.175	0.714	0.717	0.591	1.000					
CaO	-0.326	0.398	0.624	0.603	0.644	1.000				
Na_2O	0.012	0.428	0.380	0.355	0.586	0.414	1.000			
K_2O	0.018	0.508	0.495	0.423	0.626	0.390	0.852	1.000		
TiO_2	0.075	0.844	0.487	0.412	0.598	0.223	0.352	0.394	1.000	
P_2O_5	0.046	0.810	0.472	0.369	0.597	0.208	0.293	0.360	0.857	1.000

Table 4 Unrotated component matrix from loadings of 10 major elements on four significant factors for 70 samples

Variable	Factor 1	Factor 2	Factor 3	Factor 4
SiO_2	0.078	-0.357	0.169	0.813
$Al2O_3$	0.746	-0.274	0.324	-0.370
Fe_2O_3T	0.561	0.731	0.123	0.280
MnO	0.478	0.761	0.171	0.345
MgO	0.908	0.171	-0.130	-0.088
CaO	0.555	0.392	-0.347	-0.396
Na_2O	0.646	-0.363	-0.572	0.149
K_2O	0.622	-0.321	-0.575	0.239
TiO_2	0.688	-0.439	0.399	-0.018
P_2O_5	0.704	-0.255	0.509	-0.060
Eigenvalues	4.012	1.991	1.391	1.243
% of Variance	40.12	19.91	13.91	12.43
Cumulative %	40.12	60.04	73.94	86.38

Table 5 Varimax rotated component loadings of 10 major elements on four significant components explaining 86.38% of the total variance

Variable	Component 1	Component 2	Component 3	Component 4
SiO_2	0.091	0.077	0.202	-0.877
Al_2O_3	0.885	0.036	0.176	0.239
Fe_2O_3T	0.104	0.960	0.060	0.073
MnO	0.050	0.977	-0.017	0.001
MgO	0.491	0.509	0.530	0.313
CaO	0.117	0.377	0.361	0.673
Na_2O	0.201	-0.007	0.926	0.001
K_2O	0.145	0.047	0.922	-0.065
TiO_2	0.868	0.018	0.215	-0.159
P_2O_5	0.883	0.170	0.077	-0.085
Eigenvalues	2.655	2.316	2.248	1.419
% of Variance	26.55	23.16	22.48	14.19
Cumulative %	26.55	49.71	72.19	86.38

Component 1 is responsible for 27% of the total variance with Al_2O_3, TiO_2 and P_2O_5 as the dominant oxides. From the correlation matrix, there exist strong and positive correlations between Al_2O_3 and TiO_2 (r=0.844); Al_2O_3 and P_2O_5 (r=0.810). The presence of TiO_2 and P_2O_5 are indicative of basaltic rocks of oceanic environments. Components 1 and 2 comprise the phyllosilcates which form building blocks for most clay minerals [11]. Component 2 which accounts for 23% of the total variance and shows high correlation between Fe_2O_3T and MnO (r=0.818), Component 3 explains 22% of the total variance consisting mainly of alkali oxides with high correlation between Na_2O and K_2O (r=.852). Component 4 contributes 14% to the total variance with SiO_2 and CaO.

The strong correlation between Fe_2O_3 and MgO (r=0.717), MnO (r=0.818) and CaO (r=0.624) indicates that these elements are present in carbonates, probably siderite as the mean for Fe_2O_3 is greater than the total of MnO + MgO + CaO.

4.2 Trace elements

25 trace elements were subjected to fusion inductively coupled plasma (FUS-ICP) and total digestion - inductively coupled plasma (TD-ICP) analyses. Out of all the samples analyzed for, Bi, Tl and W were below the detection limit and were thus excluded from further analysis (Table 6). The Spearman's was applied to determine the correlation coefficient between trace elements (Table 7). Correlation matrix was further applied in FA. The initial application of FA produced overlap in factors for Y and Ag (Table 8). Rotation of the axis of the initial factors after 12 iterations produced a new set of factors (Table 9). With the exception of Pb, the other elements produced minimal overlap, indicating dual sources contributing to the presence of Pb.

Table 6: Descriptive statistics of trace elements

Variable N=70	Min	Max	Mean	S.D.
		(ppm)		
Ba*(1)	1.00	843.00	297.94	208.63
Sr*(1)	1.00	179.00	52.43	34.66
Y*(4)	0.50	87.00	30.11	18.87
Sc*(5)	0.50	22.00	9.32	6.29
Zr	2.00	6257.00	740.39	840.45
Be*(23)	0.50	6.00	1.78	1.25
V*(4)	2.50	155.00	66.54	46.54
Ag*(10)	0.15	2.50	0.85	0.48
As*(32)	1.50	27.00	4.33	4.40
Cd*(35)	0.15	0.90	0.30	0.18
Co* (10)	0.50	45.00	13.83	11.91
Cr	4.00	156.00	58.84	40.13
Cu*(4)	0.50	74.00	15.76	12.73
Ga	1.00	28.00	11.41	7.11
Hg*(39)	0.50	6.00	1.01	0.88
Mo*(31)	0.50	3.00	1.24	0.80
Ni*(1)	0.50	65.00	19.78	15.23
Pb*(2)	1.50	77.00	23.37	13.65
Sb*(65)	2.50	11.00	2.87	1.36
S*(%)(14)	0.005	3.08	0.43	0.78
Te *(49)	1.00	24.00	2.69	3.88
Zn	5.00	235.00	48.04	42.94

** Variables with samples below detection limit, Min value is half the D.L value*
( ) Number of samples below detection limit

Components 1 and 2 explain 52% of the total variance for trace elements in the dataset and accounts for majority of the analysed trace elements. The inferred host phases for component 1 are a mixture of lithophiles (Sc, Be, V, and Cr; with r = 0.699-0.986), chalcophiles (Cd, Cu, Ga, Te and Zn; with r = 0.561-0.751) and siderophile (Co, Mo and Ni; with high r = 0.820-0.906). Component 2 has a combination of lithophiles (Y and Zr) and chalcophile (Ag). The first two

components indicate the different sources of trace elements in the Maastichtian coal measures. Component 3 accounts for 11% of the total variance and is made up of lithophiles (Ba and Sr) while components 4, 5 and 6 comprise mainly of chalcophiles.

Table 7: Correlation matrix of trace elements

	Ba	Sr	Y	Sc	Zr	Be	V	Ag	As	Cd	Co	Cr	Cu	Ga	Hg	Mo	Ni	Pb	Sb	S	Te	Zn
Ba	1.000																					
Sr	.843	1.000																				
Y	.458	.678	1.000																			
Sc	.487	.691	.855	1.000																		
Zr	.146	.128	.408	.149	1.000																	
Be	.427	.565	.481	.699	-.264	1.000																
V	.487	.692	.825	.986	.103	.738	1.000															
Ag	.438	.499	.614	.501	.618	.167	.491	1.000														
As	.162	.260	.244	.323	-.034	.267	.322	.109	1.000													
Cd	.456	.554	.502	.699	-.136	.715	.703	.218	.308	1.000												
Co	.668	.687	.545	.711	-.066	.711	.739	.397	.219	.720	1.000											
Cr	.444	.643	.735	.923	.037	.745	.935	.469	.268	.693	.727	1.000										
Cu	.550	.649	.492	.698	-.217	.741	.729	.208	.205	.751	.745	.784	1.000									
Ga	.468	.667	.687	.908	-.080	.775	.930	.376	.341	.667	.735	.926	.752	1.000								
Hg	.297	.464	.499	.600	-.089	.567	.617	.148	.273	.429	.423	.588	.478	.654	1.000							
Mo	.495	.567	.545	.692	-.080	.690	.736	.307	.258	.746	.758	.698	.711	.734	.469	1.000						
Ni	.603	.692	.565	.768	-.131	.801	.807	.362	.307	.766	.943	.820	.820	.830	.561	.765	1.000					
Pb	.497	.733	.795	.907	.114	.648	.913	.481	.261	.667	.718	.906	.727	.876	.615	.667	.784	1.000				
Sb	-.198	-.223	-.244	-.174	-.165	-.056	-.156	-.216	-.086	-.219	-.149	-.081	-.061	-.021	.074	-.090	-.095	-.203	1.000			
S	.434	.348	.012	.063	-.296	.426	.132	.044	.136	.464	.525	.170	.493	.200	.119	.471	.524	.144	.041	1.000		
Te	.408	.369	.342	.508	-.010	.475	.519	.316	.243	.561	.585	.500	.397	.484	.267	.504	.561	.447	-.196	.285	1.000	
Zn	.685	.717	.623	.778	.013	.769	.788	.433	.224	.751	.902	.749	.737	.760	.507	.704	.881	.745	-.239	.391	.587	1.000

Table 8: Unrotated component matrix from loadings of 22 trace elements on six significant factors for 70 samples

Variable	Factor 1	Factor 2	Factor 3	Factor 4	Factor 5	Factor 6
Ba	0.580	0.120	0.407	0.427	-0.275	0.091
Sr	0.748	0.186	0.046	0.413	-0.326	0.085
Y	0.736	0.609	0.022	0.003	0.130	0.068
Sc	0.934	0.173	-0.184	-0.152	0.035	-0.030
Zr	-0.036	0.836	0.123	-0.170	0.369	0.104
Be	0.766	-0.324	-0.161	-0.022	-0.027	-0.024
V	0.942	0.084	-0.187	-0.151	0.043	-0.040
Ag	0.518	0.670	0.219	0.017	0.125	0.046
As	0.319	-0.135	-0.066	-0.331	-0.148	0.783
Cd	0.797	-0.298	0.167	-0.161	0.003	0.095
Co	0.857	-0.151	0.292	-0.002	0.092	-0.144
Cr	0.914	0.071	-0.255	-0.082	-0.009	-0.171
Cu	0.709	-0.196	-0.086	0.148	-0.093	-0.216
Ga	0.904	-0.068	-0.318	-0.011	0.032	-0.022
Hg	0.476	-0.063	-0.532	0.182	0.041	0.351
Mo	0.786	-0.199	0.089	0.146	0.184	0.043
Ni	0.912	-0.157	0.103	0.047	0.078	-0.097
Pb	0.859	0.292	-0.130	0.173	-0.062	-0.065
Sb	-0.189	-0.234	-0.430	0.284	0.596	-0.026
S (%)	0.195	-0.401	0.517	0.336	0.450	0.289
Te	0.514	-0.223	0.288	-0.462	0.139	-0.165
Zn	0.790	-0.245	0.209	-0.283	-0.017	-0.011
Eigenvalues	11.059	2.366	1.514	1.167	1.017	1.006
% of Variance	50.27	10.75	6.88	5.30	4.62	4.57
Cumulative %	50.27	61.02	67.90	73.21	77.83	82.40

Table 9: Varimax rotated component loadings of 22 trace elements on six significant components explaining 820.40% of the total variance

Variable	Component 1	Component 2	Component 3	Component 4	Component 5	Component 6
Ba	0.288	0.142	0.739	0.278	0.009	-0.235
Sr	0.461	0.170	0.792	-0.002	0.103	-0.024
Y	0.490	0.756	0.335	-0.054	0.096	0.005
Sc	0.853	0.365	0.217	-0.140	0.181	0.045
Zr	-0.212	0.909	-0.130	-0.046	-0.025	-0.022
Be	0.790	-0.140	0.185	0.045	0.172	0.097
V	0.887	0.290	0.197	-0.108	0.180	0.057
Ag	0.260	0.779	0.300	0.032	-0.003	-0.132
As	0.178	0.015	0.011	0.079	0.907	-0.089
Cd	0.776	-0.025	0.132	0.263	0.260	-0.170
Co	0.814	0.121	0.237	0.324	-0.046	-0.176
Cr	0.886	0.220	0.238	-0.195	0.059	0.096
Cu	0.704	-0.100	0.334	0.004	-0.075	0.059
Ga	0.868	0.114	0.250	-0.105	0.187	0.223
Hg	0.369	0.015	0.260	-0.118	0.431	0.517
Mo	0.712	0.076	0.267	0.343	0.090	0.109
Ni	0.861	0.097	0.287	0.226	0.027	-0.024
Pb	0.675	0.378	0.504	-0.120	0.035	0.097
Sb	-0.057	-0.107	-0.259	0.167	-0.148	0.762
S (%)	0.108	-0.066	0.091	0.911	0.053	0.090
Te	0.644	0.051	-0.265	0.205	0.020	-0.356
Zn	0.806	0.020	0.052	0.197	0.192	-0.283
Eigenvalues	9.036	2.555	2.442	1.482	1.310	1.303
% of Variance	41.07	11.61	11.10	6.74	5.96	5.92
Cumulative %	41.07	52.69	63.78	70.52	76.48	82.40

5. Conclusion

The Maastrichtian coal measures in the Anambra Basin were investigated for their geochemical elemental associations0. Geochemical analyses have shown through statistical correlation of major and trace element contents that the coals and non-coal strata belong to two distinct unrelated populations0. The first population is clearly derived from the clastic rocks in the sequence0. It represents a simple, two end-member mixing model0. One of the end members is nearly pure quartz (960.4 % SiO_2) with very minute amounts of the trace elements0. The other end member has minor amounts of clay and perhaps accessory detrital minerals and accounts for the majority of the trace elements0.

The second population comprises the coal samples0. The trends of these coal samples are fairly typical - the higher the ash yield, the higher the element concentrations0. The two suits are unrelated because there is no transition from one to the other in any of the diagrams0. There is a gap with no ash yield values between about 35 to 60%0. The first suite represents periodic flooding and killing of the peat swamp from a source that is not the regular source of detritus particles deposited in the peat swamp0. However, it is therefore recommended that further studies and more detailed stratigraphic and geochemical analyses be carried out within the study area0.

Acknowledgements

The service rendered by the Geological Survey Agency of Nigeria, Kaduna, is acknowledged in the provision of core samples used in this study0. The authors are also grateful to the Activation Laboratories, Ontario, Canada, for the analysis of the entire samples

References

[1] Obaje, N. G., Ulu, O. K. and Petters,S. W.: NAPE Bull 1999, 14, 18-540.
[2] Reyment,R.A.: In: Aspects of the Geology of Nigeria, University of Ibadan Press, Ibadan, 1965, p. 1450.
[3] Wright, J. B., Hastings, D.A., Jones, W. B. and Williams, H. R.: Geology and Mineral Resources of West Africa, Allen and Unwin, London, 1985, p. 187.
[4] Ndiokwere, C. L., Guinn , V. P.and Burtner, D.: J. Radioanalytical and Nuclear Chemistry 1983, 79, 123-128.
[5] Olabanji, S. O.: J. Radioanalytical and Nuclear Chemistry 1991, 149, 41-49.
[6] Ewa,I. O. B.: Applied Radiation and Isotopes 2004, 60, 751-758.
[7] Olajire, A. A., Ameen, A. B., Abdul-Hammed M. and Adekola, F. A.: Journal of Fuel Chemistry and Technology 2007, 35, 641-647.
[8] Ehinola, O. A. and Adene, T. M.: Petroleum & Coal 2008, 50, 19-26.
[9] Cristache, C. I., Duliu, O. G., Culicov, O.A., Frontasyeva, M. V., Ricman, C. and Toma, M.: Applied Radiation and Isotopes 2009, 67, 901-906.
[10] Liu, C.-W, Lin, K.-H and Kuo, Y.-M: Science of the Total Environment 2003, 313, 77-89.
[11] Horner, T. C. and Krissek, L. A.: In Statistical analysis of geochemical patterns in fine-grained Permian clastics from the Beardmore Glacier region, Antarctica, Vol0. Eds.: Y. Yoshida, K Kaminuma and K. Shiraishi), TERRAPUB, Tokyo, Japan, 1992, pp0. 241-248.